



**HELMHOLTZ  
ZENTRUM FÜR  
INFEKTIONSFORSCHUNG**

**This is a postprint of an article published in  
Walker, M.J., Hollands, A., Sanderson-Smith, M.L., Cole, J.N., Kirk, J.K.,  
Henningham, A.,  
McArthur, J.D., Dinkla, K., Aziz, R.K., Kansal, R.G., Simpson, A.J.,  
Buchanan, J.T.,  
Chhatwal, G.S., Kotb, M., Nizet, V.  
DNase Sda1 provides selection pressure for a switch to invasive group A  
streptococcal infection  
(2007) Nature Medicine, 13 (8), pp. 981-985.**

**DNase Sda1 Provides Selection Pressure for a Genetic and  
Phenotypic Switch Promoting Invasive Group A Streptococcal  
Infection**

Mark J. Walker<sup>1\*</sup>, Andrew Hollands<sup>1</sup>, Martina L. Sanderson-Smith<sup>1</sup>, Jason N. Cole<sup>1</sup>,  
Joshua K. Kirk<sup>1</sup>, Anna Henningham<sup>1</sup>, Jason D. McArthur<sup>1</sup>, Katrin Dinkla<sup>2</sup>, Ramy K.  
Aziz<sup>3,4</sup>, Rita G. Kansal<sup>4,5</sup>, Amelia J. Simpson<sup>6</sup>, John T. Buchanan<sup>6</sup>, Gursharan S.  
Chhatwal<sup>2</sup>, Malak Kotb<sup>4,5</sup>, Victor Nizet<sup>6,7</sup>

<sup>1</sup>School of Biological Sciences, University of Wollongong, Wollongong, New South Wales 2522, Australia; <sup>2</sup>Department of Microbial Pathogenesis and Vaccine Development, Helmholtz Centre for Infection Research, Braunschweig D-38124, Germany; <sup>3</sup>Department of Microbiology and Immunology, Cairo University, Cairo, Egypt; <sup>4</sup>The VA Medical Center and <sup>5</sup>The MidSouth Center for Biodefense and Security, Memphis, Tennessee 38163, USA; <sup>6</sup>Department of Pediatrics and <sup>7</sup>Skaggs School of Pharmacy & Pharmaceutical Sciences, UCSD, La Jolla, California 92093-0687, USA.

\*Corresponding author: Professor Mark J. Walker, School of Biological Sciences, University of Wollongong, Wollongong, NSW, 2522, Australia. Tel: 0061-2-4221 3439; Fax: 0061-2-4221 4135; E-mail: mwalker@uow.edu.au

Most invasive bacterial infections are caused by species that more commonly colonize the human host with minimal symptoms. Although phenotypic or genetic correlates underlying a bacterium's shift to enhanced virulence have been studied, the *in vivo* selection pressure governing such shifts are poorly understood. The globally disseminated M1T1 clone of group A *Streptococcus* (GAS) is linked with rare but life-threatening syndromes of necrotizing fasciitis and toxic shock syndrome<sup>1</sup>. Mutations in the GAS control of virulence regulatory sensor kinase (*covRS*) operon are associated with severe invasive disease, abolishing expression of a broad spectrum cysteine protease (SpeB)<sup>2,3</sup> and allowing the recruitment and activation of host plasminogen on the bacterial surface<sup>4</sup>. Here we describe how bacteriophage-encoded GAS DNase (Sda1), which facilitates the pathogen's escape from neutrophil extracellular traps (NETs)<sup>5,6</sup>, serves as a selective force for *covRS* mutation. The results provide a paradigm whereby natural selection exerted by the innate immune system generate hypervirulent bacterial variants with increased risk of systemic dissemination.

GAS is estimated to cause ~700 million cases of self-limited throat or skin infection each year worldwide<sup>7</sup>. Invasive GAS disease occurs in approximately 1/1,000 cases, with associated mortality of 25%<sup>7</sup>. Epidemic invasive disease is associated with the emergence of the globally disseminated GAS M1T1 clone<sup>1,8</sup>, which is distinguished from related strains by acquisition of prophages encoding virulence determinants such as superantigen SpeA and DNase Sda1<sup>9,10</sup>. In the M1T1 GAS clone, the transition from local to systemic infection can be linked to mutations in the two-component *covRS* regulator. The effect of these mutations is a distinct shift in the transcriptional

profile of invasive GAS isolates compared to mucosal (throat) isolates<sup>3</sup>. The *covRS* mutation and changes in gene expression are recapitulated upon subcutaneous challenge of mice and analysis of GAS disseminating to the spleen in comparison with those in the original inoculum<sup>3</sup>. Prominent changes in the transcriptional profile of invasive GAS isolates include a strong up-regulation of the DNase gene *sda1*, and a marked decrease in expression of the gene encoding the cysteine protease SpeB<sup>3</sup>. Sda1 is a virulence factor that protects GAS against neutrophil killing by degrading the DNA framework of NETs<sup>5,6</sup>. Abolishment of SpeB expression allows accumulation and activation of the broad spectrum host protease plasmin on the GAS bacterial surface<sup>4</sup>. A clinical correlation of GAS invasive disease severity and diminished SpeB expression has been established<sup>2</sup>.

To elucidate the selection pressure for the rapid loss of SpeB expression *in vivo*, we have compared the human MIT1 GAS isolate 5448 and its isogenic animal passaged SpeB-negative variant 5448AP<sup>11</sup>. DNA sequence analysis shows 5448AP contains a single adenine base insertion at position 877 of the *covS* gene (**Fig. 1a**) and lacks SpeB production (**Fig. 1b**). Whilst equivalent to wild-type (WT) 5448 in expression of plasminogen receptors  $\alpha$ -enolase<sup>12</sup> and GAPDH<sup>13</sup>, 5448AP exhibits higher levels of the fibrinogen-binding M1 protein<sup>14,15</sup> and streptokinase (**Fig. 1c**). Although washed 5448 and 5448AP cells bind identical levels of human plasminogen (**Fig. 1d**), 5448AP accumulates significantly higher levels of surface plasmin activity following growth in human plasma ( $P < 0.05$ ; **Fig. 1e**). The observed phenotypes of 5448AP parallel those seen upon allelic replacement of the *speB* gene in the parent strain (mutant 5448 $\Delta$ *speB*<sup>4</sup>), indicating that surface plasmin acquisition by 5448AP reflects the loss of SpeB. Additionally, other gene expression changes, such as the increase in

streptokinase expression associated with *covRS* mutation<sup>3</sup>, may also contribute to surface plasmin acquisition by 5448AP (**Supplementary Fig. 1**). Compared to WT, the 5448AP strain was found to be hypervirulent in a humanized plasminogen mouse subcutaneous infection model ( $P < 0.05$ ; **Fig. 1f** and **Supplementary Fig. 2**). Isogenic mutagenesis of 5448AP was undertaken to construct a streptokinase-deficient strain (5448AP $\Delta$ *ska*), which showed reduced virulence in comparison to 5448AP ( $P < 0.05$ ; **Fig. 1f**). This observation is consistent with the reduced virulence of *ska*-deficient GAS previously reported<sup>16</sup>. Enumeration of bacterial counts in the site of infection, blood, spleen and liver of humanized plasminogen mice, suggest that the enhanced virulence of strain 5448AP is as a result of a widespread systemic infection following breakout from the site of local infection, immediately prior to the death of the mice (**Fig. 1g**). These humanized animal model data reflect observations made in the clinical setting for GAS MIT1 strains, where mutations in *covRS* correlate with human invasive disease severity<sup>2,3</sup>.

Next, infection chambers were implanted subcutaneously in mice and inoculated with either GAS 5448 or 5448AP. After 24 h, bacteria were recovered and analyzed for SpeB and Sda1 expression. Quantitative real-time PCR analysis reveals *speB* expression is down-regulated over 10,000 $\times$  in 5448AP, when compared to WT 5448 (**Fig. 2a**). In contrast, an over 5 $\times$  up-regulation of *sda1* gene expression was observed by 24 h in 5448 following *in vivo* growth, which matched the increased DNase expression levels seen *in vivo* for 5448AP (**Fig. 2b** and **Supplementary Fig. 3a**). DNA degradation by 5448AP was increased compared to the GAS 5448 parent strain (**Fig. 2c** and **Supplementary Fig. 3b**), consistent with both the up-regulation of *sda1* expression and the known ability of SpeB to degrade Sda1<sup>11</sup>. Compared to the 5448

parent strain, the enhanced DNase activity of 5448AP was associated with clearance of NETs (**Fig. 2d** and **Supplementary Fig. 4a**) and increased resistance to neutrophil killing (**Fig. 2e**). Neither streptokinase nor M1 protein contribute to NET clearance (**Supplementary Fig. 4b**).

Neutrophils and NET-mediated extracellular killing play a pivotal role in antibacterial clearance at the initial site of infection<sup>5,17</sup>. We hypothesized that acquisition of the potent bacteriophage-encoded DNase Sda1 by the MIT1 clone provides the selective force for loss of SpeB expression *in vivo*, since the cysteine protease is capable of degrading this important neutrophil survival factor. To examine this possibility, we subcutaneously challenged C57BL/J6 mice separately with 5448 and the isogenic 5448 $\Delta$ *sda1* mutant, predicting that absence of Sda1 would reduce the selective advantage for mutation to a SpeB-negative phenotype. Loss of SpeB expression *in vivo* during subcutaneous mouse infection was abrogated in the isogenic 5448 $\Delta$ *sda1* mutant compared to WT 5448 (**Fig. 2f**; 1/500 SpeB-negative 5448 $\Delta$ *sda1* colony versus 76/500 SpeB-negative 5448 colonies;  $P < 0.05$ ). DNA sequence analysis of 10 selected SpeB-negative 5448 colonies suggests that mutations in *covRS* have resulted in loss of SpeB expression (**Supplementary Table 1**), as previously reported<sup>3</sup>. We used reverse complementation to replace the mutated chromosomal locus in 5448 $\Delta$ *sda1* with the WT allele to construct 5448RC*sda1*<sup>+</sup>. This complemented mutant regained the capacity to switch to the SpeB-negative phenotype (**Fig. 2f**; 45/500 SpeB-negative 5448RC*sda1*<sup>+</sup> colonies;  $P = 0.39$ ). The isogenic mutant 5448 $\Delta$ *smez*, derived in a manner identical to 5448 $\Delta$ *sda1*, was found to retain the capacity to phase-switch similar to the WT strain 5448 (**Fig. 2f**; 33/500 SpeB-negative 5448 $\Delta$ *smez* colonies;  $P = 0.11$ ). These observations suggest that the phase-switching phenotype is

due to allelic replacement of the *sdal* gene and not due to the methodology used to construct an isogenic GAS mutant in strain 5448. The M1 serotype GAS strain SF370 is known not to encode Sda1<sup>9,10</sup>. SF370 was found to have minimal capacity to switch to the SpeB-negative phenotype compared to 5448 (**Fig. 2f**; 2/500 SpeB-negative SF370 colonies;  $P < 0.05$ ) consistent with the absence of Sda1 and thus lack of selective advantage for mutation to the SpeB-negative phenotype.

The globally disseminated *Streptococcus pyogenes* MIT1 clone emerged in the mid-1980s as a major cause of severe GAS invasive disease. Recent genome-scale analyses have found that in comparison to other M1 strains, the MIT1 clone has acquired two lysogenised bacteriophage genomes encoding Sda1 and SpeA, respectively<sup>9,10</sup>. While the introduction of SpeA into the GAS population increases the propensity to cause streptococcal toxic shock, this study has shown that positive selection pressure *in vivo* is placed upon the bacteriophage-encoded virulence determinant Sda1. Loss of SpeB spares Sda1 from degradation<sup>11</sup> and improves GAS resistance against neutrophil clearance. *In vivo*, the phase-shift in SpeB expression is abrogated by isogenic mutagenesis of *sdal*. The genetic basis for loss of SpeB expression has been previously described<sup>3</sup>. Loss of SpeB has also been shown to result in increased invasive propensity of MIT1 by the accumulation of surface-bound plasmin activity<sup>4</sup>. Therefore, we hypothesize that the bacteriophage-mediated acquisition of the *sdal* gene by the ancestral MIT1 has provided evolutionary selection pressure for increased neutrophil resistance via SpeB loss, which results in a hyperinvasive phenotype and can lead to severe invasive disease progression (**Fig. 3**). The evolution of bacterial pathogens principally occurs either through deletion events or horizontal gene transfer and acquisition<sup>18</sup>, which is exemplified by the

bacteriophage-mediated acquisition of the *sdal* gene by MIT1. These data provide a paradigm for bacteriophage-mediated acquisition of virulence determinants and development of severe disease by otherwise benign human pathogens.

***Acknowledgements:***

The authors wish to thank A. Jeng and K. Chalasani for constructing the isogenic mutant 5448 $\Delta$ *smez*, and R. Attia for assisting with real-time PCR. A. Hollands and A. Henningham are recipients of an Australian Postgraduate Award. This work was supported by the National Health and Medical Research Council of Australia 459103 (MJW), National Institutes of Health (USA) Grant AI48176 (VN) and a Department of Employment Science and Technology (Australia) International Science Linkages grant CG001195 (MJW, VN, MK). The authors thank G. Ellmers and R. Dinnervill for illustrating Fig. 3, and M. Wilson for critically reading this manuscript.



**References:**

1. Cunningham, M.W. Pathogenesis of group A streptococcal infections. *Clin. Microbiol. Rev.* **13**, 470–511 (2000).
2. Kansal, R.G., McGeer, A., Low, D.E., Norrby-Teglund, A. & Kotb, M. Inverse relation between disease severity and expression of the streptococcal cysteine protease, SpeB, among clonal M1T1 isolates recovered from invasive group A streptococcal infection cases. *Infect. Immun.* **68**, 6362–6369 (2000).
3. Sumbly, P., Whitney, A.R., Graviss, E.A., DeLeo, F.R. & Musser, J.M. Genome-wide analysis of group A streptococci reveals a mutation that modulates global phenotype and disease specificity. *PLoS Pathog.* **2**, 41–49 (2006).
4. Cole, J.N. *et al.* Trigger for group A streptococcal M1T1 invasive disease. *FASEB J.* **20**, 1745–1747 (2006).
5. Buchanan, J.T. *et al.* DNase expression allows the pathogen group A *Streptococcus* to escape killing in neutrophil extracellular traps. *Curr. Biol.* **16**, 396–400 (2006).
6. Sumbly, P. *et al.* Extracellular deoxyribonuclease made by group A *Streptococcus* assists pathogenesis by enhancing evasion of the innate immune response. *Proc. Natl Acad. Sci. USA* **102**, 1679–1684 (2005).
7. Carapetis, J.R., Steer, A.C., Mulholland, E.K. & Weber, M. The global burden of group A streptococcal diseases. *Lancet Infect. Dis.* **5**, 685–694 (2005).
8. Walker, M.J., McArthur, J.D., McKay, F.C. & Ranson, M. Is plasminogen deployed as a *Streptococcus pyogenes* virulence factor? *Trends Microbiol.* **13**, 308–313 (2005).
9. Aziz, R.K. *et al.* Mosaic Prophages with horizontally acquired genes account for the emergence and diversification of the globally disseminated M1T1 clone of *Streptococcus pyogenes*. *J. Bacteriol.* **187**, 3311–3318 (2005).
10. Sumbly, P. *et al.* Evolutionary origin and emergence of a highly successful clone of serotype M1 group A *Streptococcus* involved multiple horizontal gene transfer events. *J. Infect. Dis.* **192**, 771–782 (2005).

11. Aziz, R.K. *et al.* Invasive M1T1 group A *Streptococcus* undergoes a phase-shift *in vivo* to prevent proteolytic degradation of multiple virulence factors by SpeB. *Mol. Microbiol.* **51**, 123–134 (2004).
12. Pancholi, V. & Fischetti, V.A. alpha-enolase, a novel strong plasmin(ogen) binding protein on the surface of pathogenic streptococci. *J. Biol. Chem.* **273**, 14503–14515 (1998).
13. Pancholi, V. & Fischetti, V.A. A major surface protein on group A streptococci is a glyceraldehyde-3-phosphate-dehydrogenase with multiple binding activity. *J. Exp. Med.* **176**, 415–426 (1992).
14. Ringdahl, U. *et al.* A role for the fibrinogen-binding regions of streptococcal M proteins in phagocytosis resistance. *Mol. Microbiol.* **37**, 1318–1326 (2000).
15. McArthur, J.D. & Walker, M.J. Domains of group A streptococcal M protein that confer resistance to phagocytosis, opsonization and protection: implications for vaccine development. *Mol. Microbiol.* **59**, 1–4 (2006).
16. Sun, H. *et al.* Plasminogen is a critical host pathogenicity factor for group A streptococcal infection. *Science* **305**, 1283–1286 (2004).
17. Brinkmann, V. *et al.* Neutrophil extracellular traps kill bacteria. *Science* **303**, 1532–1535 (2004).
18. Ochman, H. & Moran, N.A. Genes lost and genes found: evolution of bacterial pathogenesis and symbiosis. *Science* **292**, 1096–1099 (2001).
19. Ferretti, J.J. *et al.* Complete genome sequence of an M1 strain of *Streptococcus pyogenes*. *Proc. Natl Acad. Sci. USA* **98**, 4658–4663 (2001).
20. Nizet, V. *et al.* Genetic locus for streptolysin S production by group A *Streptococcus*. *Infect. Immun.* **68**, 4245–4254 (2000).
21. Maguin, E., Duwat, P., Hege, T., Ehrlich, D. & Gruss, A. New thermosensitive plasmid for Gram-positive bacteria. *J. Bacteriol.* **174**, 5633–5638 (1992).
22. Ashbaugh, C.D., Warren, H.B., Carey, V.J. & Wessels, M.R. Molecular analysis of the role of the group A streptococcal cysteine protease, hyaluronic acid capsule, and M protein in a murine model of human invasive soft-tissue infection. *J. Clin. Invest.* **102**, 550–560 (1998).
23. Collin, M. & Olsen, A. Generation of a mature streptococcal cysteine proteinase is dependent on cell wall-anchored M1 protein. *Mol. Microbiol.* **36**, 1306–1318 (2000).

24. McKay, F.C. *et al.* Plasminogen binding by group A streptococcal isolates from a region of hyperendemicity for streptococcal skin infection and a high incidence of invasive infection. *Infect. Immun.* **72**, 364–370 (2004).
25. Kazmi, S.U. *et al.* Reciprocal, temporal expression of SpeA and SpeB by invasive MIT1 group A streptococcal isolates *in vivo*. *Infect. Immun.* **69**, 4988–4995 (2001).
26. Aziz, R.K., Ismail, S.A., Park, H.W. & Kotb, M. Post-proteomic identification of a novel phage-encoded streptodornase, Sda1, in invasive MIT1 *Streptococcus pyogenes*. *Mol. Microbiol.* **54**, 184–197 (2004).

***Figure legends:***

**Fig. 1.** Molecular and phenotypic analyses of GAS strains 5448 and 5448AP. **(a)** DNA sequence comparison of GAS strains 5448 and 5448AP confirms the presence of a 1 base adenine addition at the 3' end of *covS* (nt position 877) encoded by 5448AP (unfilled arrowhead). Primers used for DNA sequence analysis are indicated by filled arrowheads (p1 to p12). This insertion mutation results in the truncation of the CovS open reading frame at amino acid 300 from the CovS methionine start codon. Putative conserved CovS domains are indicated in lower panel: HAMP: Histidine kinases/adenylyl cyclases/methyl-binding proteins/phosphatases; HisKA, Histidine kinase domain (phosphoaceptor); HATPase: Histidine kinase-like ATPase. Scales, in base pairs (bp; upper panel bar) and amino acids (aa; lower panel bar), are indicated. **(b)** In comparison to GAS strain 5448, secreted SpeB protease activity is abrogated in 5448AP ( $n = 3$ ; mean  $\pm$  SD). Asterisk indicates statistically significant difference from 5448, where  $P < 0.05$ . **(c)** Western blot analysis of cell wall extracts indicates that equivalent amounts of  $\alpha$ -enolase (unfilled arrowhead) and GAPDH (unfilled arrowhead) are produced by strains 5448 and 5448AP, whereas higher amount of M1 protein (unfilled arrowhead) is produced in cell wall extracts and streptokinase (unfilled arrowhead) is secreted into culture supernatants by strain 5448AP, in comparison to 5448. Molecular mass markers (MWT) are given in kilo-Daltons (kDa). **(d)** Washed 5448 and 5448AP cells bind equivalent amounts of human plasminogen ( $n = 3$ ; mean  $\pm$  SD). **(e)** Following overnight growth at 37 °C in human plasma, 5448AP accumulates significantly higher levels of surface plasmin activity ( $n = 3$ ; mean  $\pm$  SD). Asterisk indicates statistically significant difference from 5448, where  $P < 0.05$ . **(f)** Survival curves following subcutaneous infection of humanized

plasminogen transgenic mice ( $n = 10$ ) with GAS strain 5448 ( $3.2 \times 10^8$  colony forming units/dose; solid line), 5448AP ( $1.6 \times 10^8$  colony forming units/dose; dashed line) and 5448AP $\Delta ska$  ( $1.5 \times 10^8$  colony forming units/dose; dotted line). (g) Enumeration of bacterial counts in the site of infection, blood, spleen and liver of humanized plasminogen mice ( $n = 5$ ) subcutaneously infected with GAS strain 5448 ( $2.6 \times 10^7$  colony forming units/dose; open circles) and 5448AP ( $4.9 \times 10^7$  colony forming units/dose; filled circles).

**Fig. 2.** Relative expression of (a) the *speB* gene and (b) the *sdaI* gene, as determined using quantitative real-time PCR ( $n = 3$ ; mean  $\pm$  SD). RNA was extracted from GAS either immediately prior to inoculation (0 h) or 24 h post-inoculation of subcutaneous infection chambers. Asterisk indicates statistically significant difference from 5448 (0 h), where  $P < 0.05$ . (c) DNase expression in GAS mid-logarithmic phase culture supernatants as assessed by degradation of calf thymus DNA (control). (d) Clearance of NETs by GAS. Neutrophils were visualized using bright field microscopy, whilst NETs were visualized using Sytox Orange staining. Scale bar = 100  $\mu$ m. (e) Killing of GAS by human neutrophils at a multiplicity of infection (GAS:neutrophils) = 1:10 ( $n = 3$ ; mean  $\pm$  SD). Asterisk indicates statistically significant difference from 5448, where  $P < 0.05$ . (f) The capacity of GAS strains 5448, 5448 $\Delta sdaI$ , 5448RC*sdaI*<sup>+</sup>, 5448 $\Delta smeZ$  and SF370 to phase-shift to a SpeB-negative phenotype was examined 3 d post-subcutaneous infection of mice.

**Fig. 3.** Model for group A streptococcal invasive disease initiation and progression. (a) Following entry via the skin, GAS (blue) are able to express SpeB (required during the early stages of the infection process; black dots). An innate immune

response is mounted by host neutrophils and entrapment of GAS in NETS (orange) begins. **(b)** Within the GAS population, a mutation in *covRS* occurs (green), resulting in loss of SpeB expression and improved resistance to killing by neutrophils. **(c)** Selection pressure by neutrophils results in an increase in the proportion of *covRS* mutant phenotype GAS within the bacterial population, improved NET clearance and neutrophil resistance. **(d)** Loss of SpeB expression allows the accumulation of surface plasmin activity leading to systemic infection.

# Figure 1

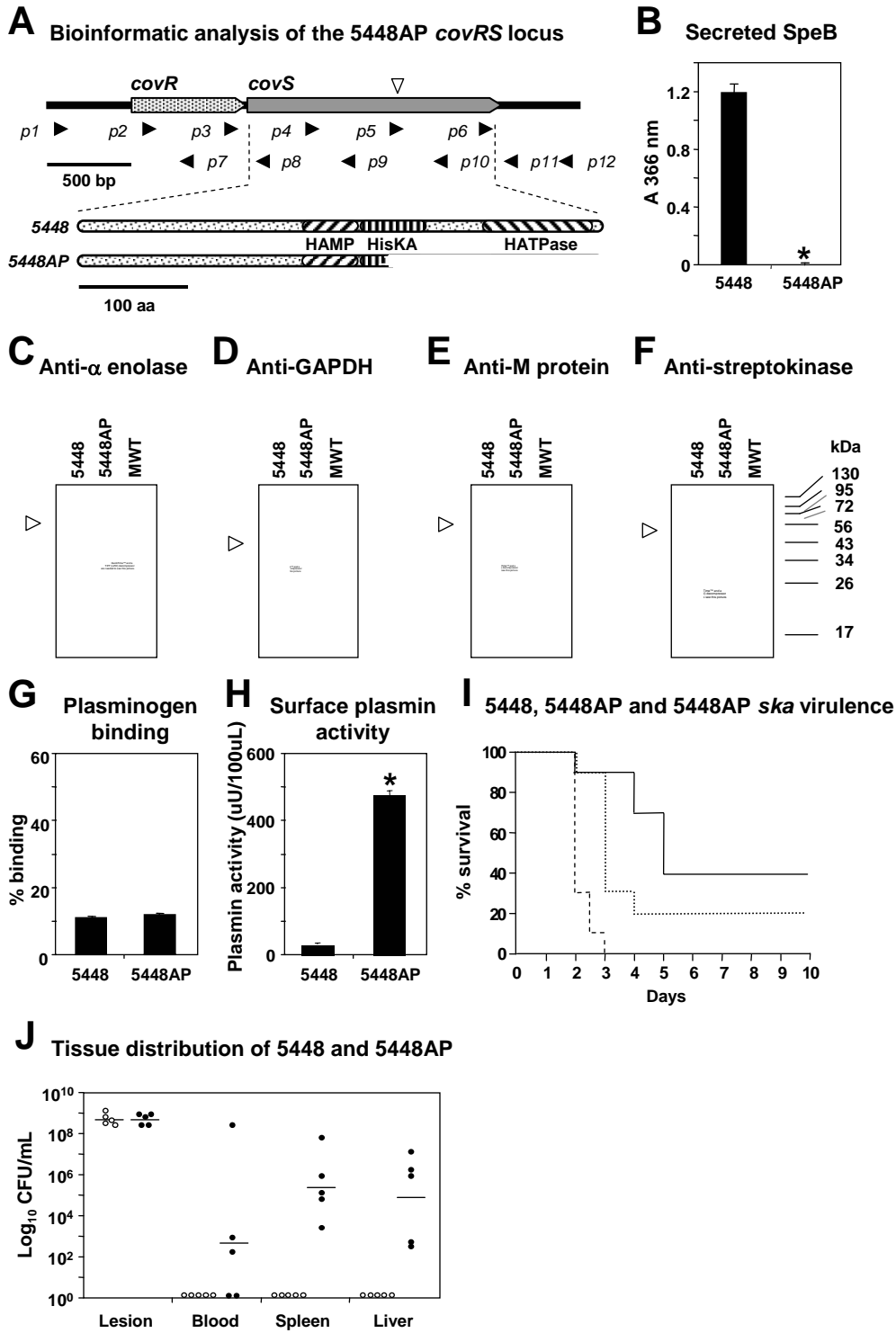


**Figure 2**

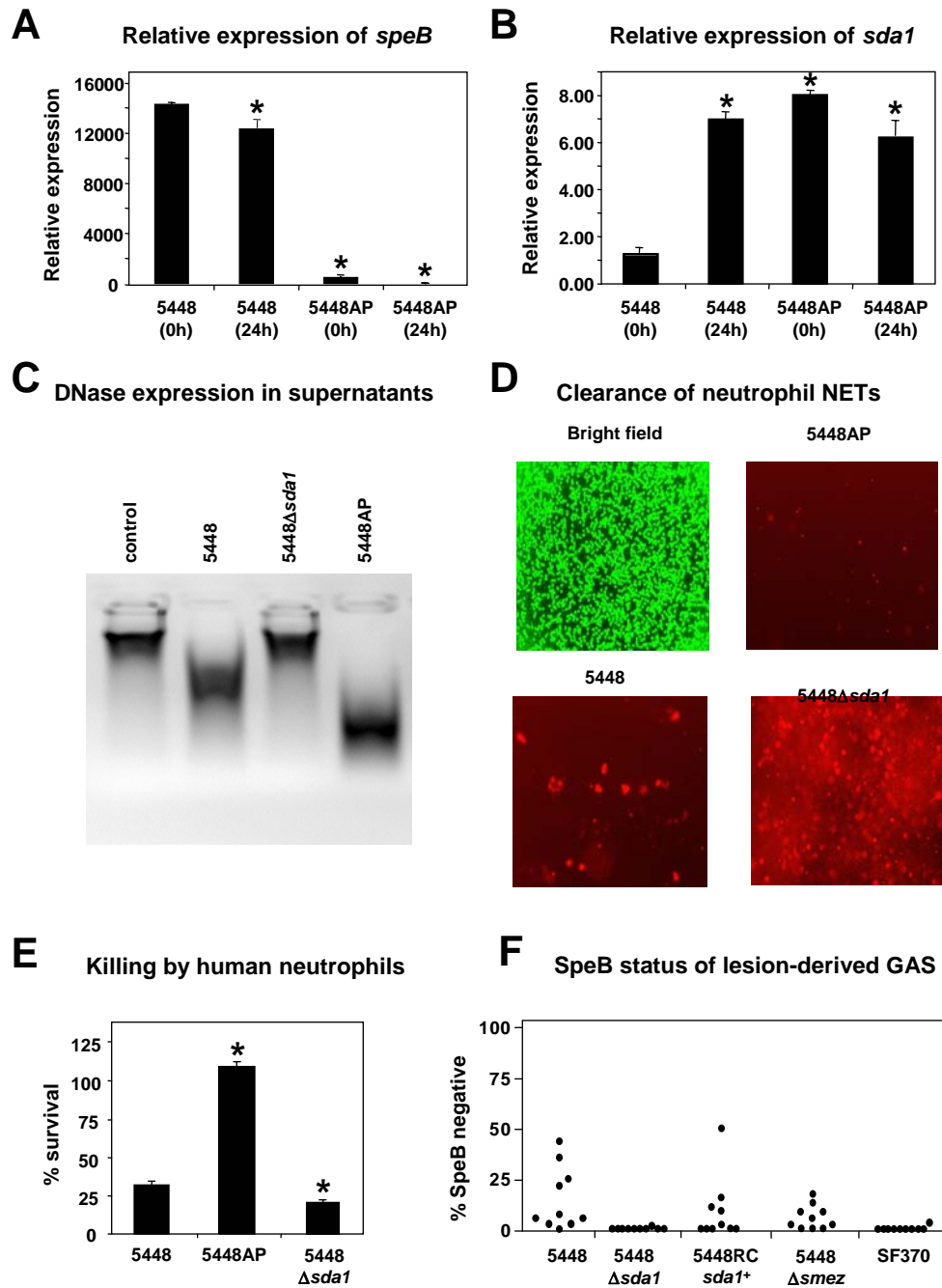
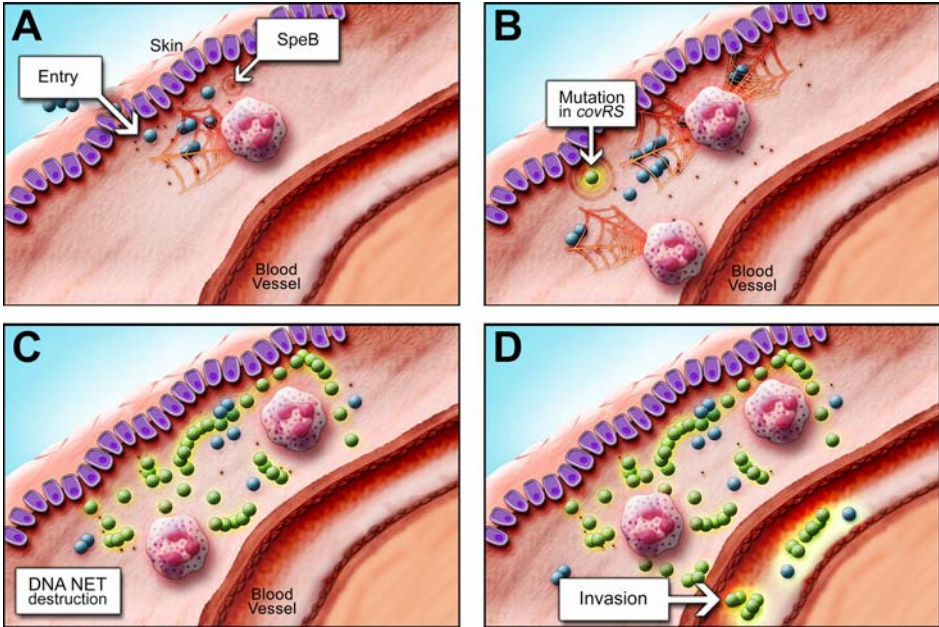


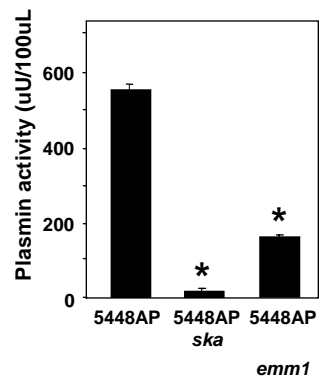


**Figure 3**



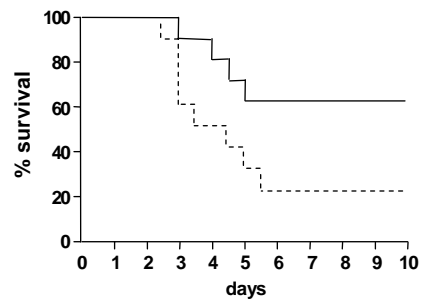
# Supplementary Figure 1

Surface plasmin activity of 5448AP, 5448AP *ska* and 5448AP *emm1*

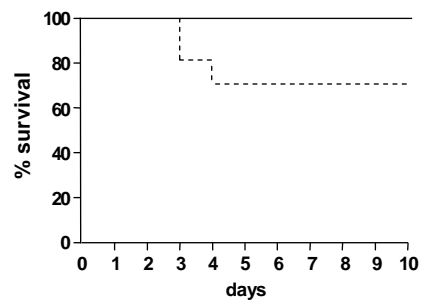


## Supplementary Figure 2

### A 5448 and 5448AP medium dose

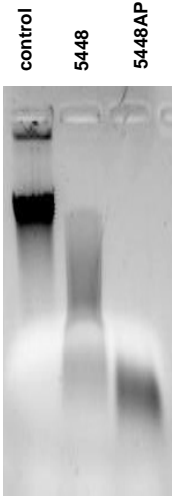


### B 5448 and 5448AP low dose

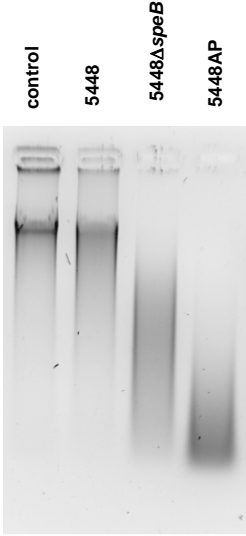


# Supplementary Figure 3

**A** DNase activity *in vivo*

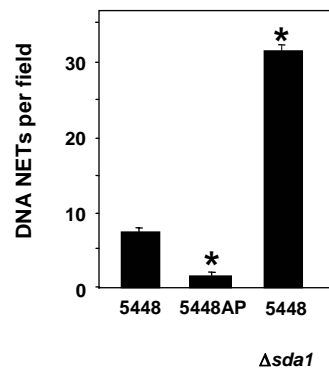


**B** Effect of SpeB

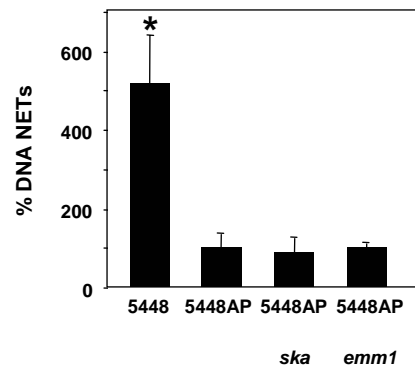


## Supplementary Figure 4

**A** Clearance of DNA NETs



**B** Effect of Ska and M1 on DNA NET clearance



**Supplementary Table 1.** *CovRS* DNA sequence analysis of selected GAS M1T1 strain 5448 SpeB-negative derivatives isolated 3 d following subcutaneous infection of C57BL/J6 mice.

<b>GAS strain</b>	<b>Mouse ID</b>	<b>Tissue<sup>a</sup></b>	<b>Mutation<sup>b</sup></b>	<b>Consequence<sup>c</sup></b>
5448-APD1	OS41B	Blood	C to T nt 838 <i>covS</i>	H to Y aa 280 <i>covS</i>
5448-APD2	OS41B	Lesion	C to T nt 838 <i>covS</i>	H to Y aa 280 <i>covS</i>
5448-APD3	OS41B	Lesion	C to T nt 838 <i>covS</i>	H to Y aa 280 <i>covS</i>
5448-APD4	OS45R	Blood	C to T nt 838 <i>covS</i>	H to Y aa 280 <i>covS</i>
5448-APD5	OS45R	Blood	C to T nt 838 <i>covS</i>	H to Y aa 280 <i>covS</i>
5448-APD6	OS46L	Lesion	Δ nt 83 <i>covS</i>	Truncation in <i>CovS</i>
5448-APD7	OS46L	Lesion	Δ nt 83 <i>covS</i>	Truncation in <i>CovS</i>
5448-APD8	OS46L	Lesion	G to A nt 331 <i>covR</i>	A to T aa 111 <i>covR</i>
5448-APD9	OS322B	Lesion	Δ nt 406-1503 <i>covS</i>	Truncation in <i>CovS</i>
5448-APD10	OS492L	Lesion	C to T nt 838 <i>covS</i>	H to Y aa 280 <i>covS</i>

<sup>a</sup>Mouse tissue from which GAS strain was isolated 3 d post-subcutaneous infection.

<sup>b</sup>Mutation positions are based upon nucleotide (nt) position in the *covR* or *covS* genes, relative to each ATG start codon.

<sup>c</sup>Substitutions in *CovR* and *CovS* are based upon amino acid (aa) position in each open reading frame, relative to each start codon.

**Supplementary Table 2.** Oligonucleotide primers used in this study for construction of recombinant GAS strains.

<b>Primer</b>	<b>Direction</b>	<b>bp</b>	<b>Sequence</b>
RCSdapHY304Fwd	Forward	29	GGGCTGCAGCTTAAACGTTGGTATTTTTA
RCSdapHY304Rev	Reverse	28	GGGGAATTCGGATAGCTTACAACCTAGTG
SdaF2	Forward	21	ATGTCTAAACATTGGAGACAT
SdaR4	Reverse	20	ATCAGATGATAAAGCAGACA
SmeZ-UpF	Forward	20	TGGCTGACAACTGTCAGGAA
SmeZ-UpR	Reverse	54	GGTGGTATATCCAGTGATTTTTTCTCCATAAATAGCCT CTTTTCAGGAGTTAT
SmeZ-DownF	Forward	54	TACTGCGATGAGTGGCAGGGCGGGGCGTAATTCATTT TTCAATATAACTTTTA
SmeZ-DownR	Reverse	20	AACGACACCTCTTTCAGCGA
Emm1-dis-F-BamHI	Forward	30	GCGGATCCTAGTCCTGACTCGCTTGGTCTA
Emm1-dis-R-XbaI	Reverse	30	GCATCTAGACTTGCAGCAAACAATCCCGCA
M1ska-dis-F-BamHI	Forward	30	GCGGATCCAACATCACAACCTGCTCACGGA
M1ska-dis-R-XbaI	Reverse		GCGTCTAGACGCGCACATGTCCCTTTAACAA
T7-For	Forward	21	GTAATACGACTCACTATAGGG
Emm1out-R	Reverse	24	GAGGTTAAGGCTAACGGTGATGGT
M1skaout-R	Reverse	24	TTGAGCCCTGGTCTGAAATCGTCA

**Supplementary Table 3.** Oligonucleotide primers used in this study for *covRS* PCR and sequence analysis.

<b>Primer</b>	<b>Direction</b>	<b>bp</b>	<b>Sequence</b>
p1	Forward	19	GCTATTCCGGTACAGGTCT
p2	Forward	19	GTCAATGGTCGTGAAGGGT
p3	Forward	22	GATGTCTATATTCGTTATCTCC
p4	Forward	22	GATGATTTTTACCACAGATAAC
p5	Forward	20	GCATATTGGTCTCTTACAAC
p6	Forward	21	GCAAATTGTAGATGGGTATCA
p7	Reverse	20	GCGGAAAATAGCACGAATAC
p8	Reverse	20	AGGCAATCAGTGTAAGGCA
p9	Reverse	21	CTTGTGCCAAATAACTCAACA
p10	Reverse	21	ATCAAAAAGCCTGCTCAAATGA
p11	Reverse	21	CTTTCATGTCATCCATCATTG
p12	Reverse	19	TTGCTCTCGTGTGCCATCT



## Supplementary Materials and Methods

**Culture of group A streptococci.** *S. pyogenes* strains were routinely propagated at 37 °C on horse blood agar (BioMérieux) or in static liquid cultures of Todd-Hewitt broth (Difco) supplemented with 1% (w/v) yeast extract (THBY). Invasive GAS isolate 5448 (M1T1) and the isogenic animal-passaged SpeB-negative variant 5448AP have been described previously<sup>11</sup>. The isogenic mutants 5448 $\Delta$ *sda1*<sup>5</sup>, 5448 $\Delta$ *speB*<sup>11</sup> and GAS strain SF370<sup>19</sup>, have also been described previously.

**Construction of recombinant GAS strains.** Allelic exchange was used to precisely replace the deleted *sda1* chromosomal locus in 5448 $\Delta$ *sda1* with the WT *sda1* gene to construct strain 5448RC*sda1*<sup>+</sup>. The technology employed to construct 5448RC*sda1*<sup>+</sup> was similar to that used in the construction of 5448 $\Delta$ *sda1*<sup>5</sup>. The PCR primers RCSdapHY304Fwd and RCSdapHY304Rev were employed for amplification of flanking DNA upstream and downstream of *sda1* in the 5448 chromosome (**Supplementary Table 2**). Following amplification, the *sda1* gene was cloned by *Pst*I/*Eco*RI digestion and T4 ligation into the temperature-sensitive plasmid pHY304<sup>5</sup>. The resulting plasmid (pHY*sda1*) was transformed into 5448 $\Delta$ *sda1* by electroporation. Integration of pHY*sda1* into the chromosome via single-crossover was achieved by culture at the permissive temperature for plasmid replication (30 °C). Following subculture at 37 °C, single-crossover chromosomal insertions were selected using chloramphenicol ( $\Delta$ *sda1*) and erythromycin (pHY304). Double-crossover was achieved by serial passage at 30 °C, and double-crossover reverse-complemented mutants were identified following removal of antibiotic selection. The reverse-complemented strain 5448RC*sda1*<sup>+</sup> was characterized as sensitive to both

chloramphenicol and erythromycin; confirmed as *sda1* PCR-positive using the forward primer SdaF2 and reverse primer SdaR4 (**Supplementary Table 2**); and able to express Sda1 upon assaying for DNase activity (as described below).

The isogenic 5448 $\Delta$ *smez* mutant was constructed in a manner identical to 5448 $\Delta$ *sda1*, as previously described<sup>5</sup>. A precise, in-frame allelic exchange replacement of the *smeZ* gene in GAS strain 5448 with a chloramphenicol acetyltransferase (*cat*) antibiotic resistance cassette was generated. The specific primer sets used for amplification of the flanking DNA upstream and downstream of *smeZ* in the 5448 chromosome are given (**Supplementary Table 2**). The primers SmeZ-UpR and SmeZ-DownF contain a 25 bp 5' extension corresponding to the 5' and 3' ends of the *cat* gene, respectively.

Integrational mutagenesis of *ska* and *emml* was performed essentially as previously described<sup>20</sup>. Internal fragments of the genes *ska* and *emml* were PCR amplified from GAS strain 5448 using specific primer pairs (**Supplementary Table 2**) and cloned by *Bam*HI/*Xba*I digestion and T4 ligation into the temperature-sensitive plasmid pVE6007<sup>21</sup>. The resultant plasmids were transformed into 5448AP by electroporation and chloramphenicol resistant transformants were grown at the permissive temperature for plasmid replication (30 °C). Single-crossover Campbell-type chromosomal insertions were selected by shifting to the non-permissive temperature (37 °C), while maintaining chloramphenicol selection. Integrational knockouts were confirmed by PCR using the forward primer T7-For and reverse primer emmlout-R or M1skaout-R (**Supplementary Table 2**). Confirmed integrational knockouts were designated 5448AP $\Delta$ *emml* and 5448AP $\Delta$ *ska*.

**Molecular and phenotypic analysis of GAS.** To screen GAS strains for mutations in the *covRS* locus, we designed 12 primers for PCR and DNA sequence analysis (**Supplementary Table 3** and **Fig. 1a**). Firstly, primers p1 and p12 were used to PCR amplify the intact *covRS* locus from genomic DNA which was extracted by phenol-chloroform. Then, an ABI PRISM 7700 Sequence Detection System (Applied Biosystems) was used to directly sequence the amplified PCR product with the 12 primers and the sequence assembled by the use of Sequencher version 4.5 (Gene Codes Corporation). Using BLASTN analysis, the assembled sequences were aligned against GAS genomes and a single adenine base insertion mutation was identified at position 877 in the 5448AP *covS* gene, using numbering relative to the ATG start codon of 5448 *covS*. Other *in vivo*-derived, SpeB-negative GAS strain 5448 derivatives were analyzed for *covRS* mutations in an identical manner.

SpeB-positive and SpeB-negative isolates were routinely identified by the Columbia skim milk agar assay<sup>22</sup>. Quantitative SpeB assays were undertaken as previously described<sup>23</sup>. Bacterial surface plasmin acquisition from human plasma assays and western blot identification of  $\alpha$ -enolase, GAPDH, streptokinase and M1 protein, were conducted essentially as previously described<sup>4</sup>, with exception that cross-specific rabbit M53 protein-specific serum was used to identify M1 protein. GAS strain NS1133<sup>24</sup> was used as an internal control for bacterial surface plasmin acquisition assays<sup>4</sup> undertaken by incubating bacteria overnight in human plasma. Plasminogen-binding assays were conducted as previously described<sup>24</sup>.

### **Virulence of GAS in a humanized plasminogen transgenic mouse model.**

Transgenic humanized plasminogen *AlbPLG1* mice heterozygous for the human plasminogen transgene<sup>16</sup> were backcrossed greater than  $n = 6$  with C57BL/6 mice (Animal Resources Centre, Perth, Australia). GAS strains 5448 and 5448AP were harvested at logarithmic phase ( $OD_{600}$  approx. 0.4), washed twice with sterile 0.7% saline and diluted to the required dose. The number of viable bacteria was determined by counting colony forming units (CFU) after plating a dilution series onto blood agar. The SpeB expression status of 5448 and 5448AP was also determined as described above ( $n = 50$ ). The 5448AP inoculum was found to be 100% SpeB-negative, while the 5448 inoculum was 100% SpeB-positive. Groups of *AlbPLG1* mice ( $n = 10$ ) were subcutaneously infected with GAS and mortality was monitored for 10 d. Alternatively, groups of *AlbPLG1* mice ( $n = 5$ ) were subcutaneously infected with either 5448 or 5448AP for 48 h and the lesion (site of infection), blood, spleen and liver harvested. Lesion, spleen and liver samples were homogenized in 2 ml of sterile 0.7% saline. The number of viable bacteria was determined by counting CFU after plating a dilution series onto blood agar.

**Isolation of mRNA and real-time PCR analysis.** In order to isolate *in vivo*-derived RNA, we utilized the subcutaneous Teflon chamber model<sup>25</sup>. Teflon chambers were inserted surgically under the skin of 6-week-old female BALB/c mice. Three weeks after surgery, tissue chamber fluid (TCF) was collected and tested for sterility. Mice that had contaminated TCF, or those that had open surgical wounds, were excluded from further experimentation. To prepare inocula, bacteria were grown overnight in THBY, checked for SpeB phenotype as detailed above, then subcultured for 18 h in THBY. Bacterial pellets were washed twice in sterile phosphate buffered saline (PBS)

and resuspended in sterile PBS to  $1 \times 10^9$  CFU/ml. We injected 100  $\mu$ l of this bacterial suspension into the subcutaneous chambers using sterile 25-gauge needles. At 24 h post-injection, sterile 25-gauge needles were used to collect the TCF to analyze bacterial content and SpeB status, and to extract RNA from recovered bacteria<sup>11, 25</sup>. This 24 h time point was chosen as WT 5448 GAS recovered from mouse infection chambers were > 95% SpeB-positive (data not shown), whereas after 3 d *in vivo* the WT subcutaneous bacterial population contain a significant proportion (up to 74%) of SpeB-negative phenotype<sup>4</sup>. 5448AP cells recovered from 24 h infection chambers were uniformly SpeB-negative. RNA was extracted from bacterial pellets using RNeasy kits (Qiagen), treated with DNase (Ambion) for 1 h to remove contaminating genomic DNA, and then recovered using RNeasy columns (Qiagen). The absence of genomic DNA in the RNA samples was confirmed by PCR using primers specific for the *speB* gene<sup>11</sup> (data not shown). The intactness and purity of isolated RNA was assessed using an Agilent Technologies Bioanalyzer (data not shown). Superscript II (Invitrogen) was used to reverse transcribe RNA into cDNA, following the manufacturer's protocol; cDNA was immediately diluted with four volumes of sterile water then aliquoted for real-time PCR reactions. We performed all Sybr-Green real-time quantitative PCR reactions using an ABI PRISM 7700 Sequence Detection System (Applied Biosystems) and calculated relative expression amounts using the delta-delta CT method<sup>11</sup>. All real-time PCR reactions were performed using biological triplicates; product specificity was confirmed by the presence of a single peak in dissociation curves. Fluorescence in all real-time quantitative PCR reactions was measured at 75 °C, a temperature at which any potential primer dimers would melt, ensuring that the PCR product measured was the

expected product. Primers used for real-time PCR analysis of *speB* and *sdal* have been previously described<sup>11, 26</sup>.

**DNase activity assays.** Supernatants were collected from mid-logarithmic ( $OD_{600} = 0.4$ ) or stationary phase cultures of GAS strains grown in THBY. Calf thymus DNA ( $1.0 \mu\text{g}/\mu\text{l}$ ) was combined with bacterial supernatant ( $2.5 \mu\text{l}$ ) in final volume of  $50 \mu\text{l}$  buffer ( $300 \text{ mM Tris}$ ,  $3 \text{ mM CaCl}_2$ ,  $3 \text{ mM MgCl}_2$ ) for 15 min at room temperature. To halt DNase activity,  $12.5 \mu\text{l}$  of  $0.33 \text{ M EDTA}$  was added to the reaction. Visualization of relative DNA degradation was undertaken by side-by-side comparison of DNA using 1% agarose gel electrophoresis.

**Live cell imaging for visualization of NETs.** NETs were visualized as previously described<sup>5</sup>. Briefly, neutrophils were seeded at  $2 \times 10^5$  per well in 96-well plates in RPMI without phenol red (Invitrogen). GAS were added to the wells at a multiplicity of infection of 1:100 (GAS:neutrophils) and Sytox Orange (Molecular Probes) added to a final concentration of  $0.1 \mu\text{M}$ . Cells were visualized without fixation or washed using a Zeiss Axiovert 100 inverted microscope with appropriate fluorescent filters, and images captured with a CCD camera. For quantitation, NETs were enumerated for each treatment by counting three fields of view after staining from three independent wells; a NET was defined as a discrete area of bright orange fluorescence larger in size than a neutrophil. Presented data are representative of experiments undertaken on three separate occasions.

**Neutrophil killing assays.** Neutrophil killing assays were performed as previously described<sup>5</sup>. Briefly, human neutrophils were isolated and purified from venous blood

using the PolyMorphPrep kit (Axis-Shield) as per the manufacturer's instructions and seeded into 96-well plates at  $2 \times 10^5$  cells/well. Logarithmic-phase bacteria grown in THBY were diluted to the desired concentration in RPMI media containing 2% heat inactivated autologous human plasma, then added to neutrophils at a multiplicity of infection of 1:10 (GAS:neutrophils). Plates were centrifuged at  $500 \times g$  for 10 min then incubated at 37 °C in 5% CO<sub>2</sub>. Following incubation for 1 h, neutrophils were lysed with 0.02% Triton X-100 and the contents of the well serially diluted and plated on Todd-Hewitt agar for overnight incubation and enumeration of CFU. Internal control wells without neutrophils were used to determine baseline bacterial counts at the assay endpoints. Percent survival of GAS was calculated as  $([\text{CFU/ml experimental well}] / [\text{CFU/ml control well}]) \times 100\%$ . All assays were performed in triplicate.

**Monitoring the *in vivo* phase-shift of GAS strains.** Separate cohorts of C57BL/J6 mice ( $n = 10$ ) were inoculated subcutaneously with a non-lethal dose of GAS to examine the *in vivo* phase-shift of SpeB during infection. The inocula used in these experiments were plated out onto blood agar plates then individual colonies tested for SpeB expression status as described above ( $n = 50$ ). The 5448, 5448 $\Delta$ *sda1*, 5448RC*sda1*<sup>+</sup> and 5448 $\Delta$ *smez* inocula were found to be 100% SpeB-positive. On day three post-infection, mice were sacrificed by CO<sub>2</sub> asphyxiation and representative bacteria isolated from skin lesions<sup>4</sup>. The SpeB status of individual colonies ( $n = 50$ ) was determined as described above.

All animal experiments were conducted according to the Guidelines for the Care and Use of Laboratory Animals (National Health and Medical Research Council,

Australia) and were approved by the University of Wollongong Animal Ethics Committee.

**Statistical analyses.** Statistical analysis of SpeB expression and status, plasminogen-binding, surface plasmin activity, quantitative real-time PCR, human neutrophil killing assays, and NET quantification were performed using a one way ANOVA with a Dunnett's Multiple Comparison Test. Differences were considered statistically significant at  $P < 0.05$ . Differences in survival of humanized plasminogen transgenic mice infected with GAS strains 5448, 5448AP and 5448AP $\Delta$ *ska* were determined by the log-rank test. All statistical tests were performed using GraphPad Prism version 4.02.